





Geophysical Research Letters[®]



RESEARCH LETTER

10.1029/2023GL103043

The Decaying Near-Surface Boundary Layer of a Retreating Alpine Glacier

Thomas E. Shaw¹ , Pascal Buri¹ , Michael McCarthy¹ , Evan S. Miles¹ , Álvaro Ayala² , and Francesca Pellicciotti^{1,3} 

¹Swiss Federal Institute, WSL, Birmensdorf, Switzerland, ²Centro de Estudios Avanzados en Zonas Áridas, La Serena, Chile,

³Institute of Science and Technology Austria (ISTA), Klosterneuburg, Austria

Key Points:

- On-glacier air temperatures have become more sensitive to ambient temperatures in a warming climate
- Up-valley winds have increased >20% between 2001 and 2021, making sensible heat fluxes more dependent on conditions outside the glacier
- The decay of the katabatic system due to glacier retreat indicates a nonlinear sensitivity of the glacier to continued warming

Supporting Information:

Supporting Information may be found in the online version of this article.

Correspondence to:

T. E. Shaw,
thomas.shaw@wsl.ch

Citation:

Shaw, T. E., Buri, P., McCarthy, M., Miles, E. S., Ayala, Á., & Pellicciotti, F. (2023). The decaying near-surface boundary layer of a retreating Alpine glacier. *Geophysical Research Letters*, 50, e2023GL103043. <https://doi.org/10.1029/2023GL103043>

Received 31 MAR 2023

Accepted 24 APR 2023

Author Contributions:

Conceptualization: Thomas E. Shaw, Pascal Buri, Francesca Pellicciotti

Data curation: Thomas E. Shaw, Francesca Pellicciotti

Formal analysis: Thomas E. Shaw, Evan S. Miles

Funding acquisition: Thomas E. Shaw, Francesca Pellicciotti

Investigation: Thomas E. Shaw, Pascal Buri, Michael McCarthy, Evan S. Miles, Álvaro Ayala, Francesca Pellicciotti

Methodology: Thomas E. Shaw, Pascal Buri, Michael McCarthy, Evan S. Miles, Álvaro Ayala, Francesca Pellicciotti

Supervision: Francesca Pellicciotti

© 2023. The Authors.

This is an open access article under the terms of the [Creative Commons Attribution License](https://creativecommons.org/licenses/by/4.0/), which permits use, distribution and reproduction in any medium, provided the original work is properly cited.

Abstract The presence of a developed boundary layer decouples a glacier's response from ambient conditions, suggesting that sensitivity to climate change is increased by glacier retreat. To test this hypothesis, we explore six years of distributed meteorological data on a small Swiss glacier in the period 2001–2022. Large glacier fragmentation has occurred since 2001 (–35% area change up to 2022) coinciding with notable frontal retreat, an observed switch from down-glacier katabatic to up-glacier valley winds and an increased sensitivity (ratio) of on-glacier to off-glacier temperature. As the glacier ceases to develop density-driven katabatic winds, sensible heat fluxes on the glacier are increasingly determined by the conditions occurring outside the boundary layer of the glacier, sealing the glacier's demise as the climate continues to warm and experience an increased frequency of extreme summers.

Plain Language Summary Down-glacier winds promote a unique micro-climate, maintaining relatively lower temperatures over the surface of mountain glaciers. Using six years of meteorological data in the period 2001–2022, we observe increases in the relative changes of above-ice air temperatures compared to temperatures outside the glacier. As the glacier ceases to develop its own micro-climate, warmer winds generated by heated valley slopes increasingly control the amount of heat transfer to melt glacier ice. This work offers new observational evidence that suggests that, as glaciers continue to shrink and fragment, they becoming increasingly sensitive to future climate warming.

1. Introduction

Near-surface air temperature (T_a) is a dominant control on the glacier surface energy balance through its influence on sensible heat fluxes, longwave radiation receipt, refreezing, and precipitation phase (Hock, 2005; Jouberton et al., 2022; Sicart et al., 2008). Accordingly, T_a is common to all types of model that aim to determine glacier surface melt and mass balance, ranging from simple degree-day approaches (e.g., Hock, 2005) and models of intermediate complexity (e.g., Jouberton et al., 2022; Litt et al., 2019; Ragettli et al., 2016) to full energy balance and land-surface model frameworks (e.g., Fugger et al., 2022; Mölg et al., 2012; Y. Wang et al., 2021). A key challenge for regional and global glacier modeling is the derivation of accurate meteorological forcing at high elevation, typically uninstrumented catchments (Chen et al., 2017; Y. Wang et al., 2021). On-glacier weather stations are rarely available, so studies often rely upon extrapolation of quantities from lower-elevation weather station observations to elevations of interest (e.g., Gabbi et al., 2014; Immerzeel et al., 2014), or on coarse resolution reanalysis or atmospheric models with generally unknown biases that may vary both altitudinally and seasonally (Scherrer, 2020; X. Wang et al., 2020).

It is typically assumed that T_a decreases linearly with elevation given a prescribed, free-air lapse rate (e.g., the moist adiabatic or “environmental” lapse rate of $-0.0065^\circ\text{C m}^{-1}$), therefore ignoring surface processes and their evolution in time and space (Karki et al., 2020). Earlier work on glacier surface energy balance and meteorology identified that these assumptions were not applicable for warm atmospheric conditions (e.g., under stable, clear sky conditions) due to the development of a glacier boundary layer and katabatic wind from the strong thermal gradient between the atmosphere and a constant 0°C surface (Greuell & Böhm, 1998; Greuell et al., 1997; Van Den Broeke, 1997). The length scale over which air parcels travel over the cool glacier surface thus significantly modifies T_a and may produce the coolest conditions toward the terminus of the glacier (Greuell & Böhm, 1998; Shea & Moore, 2010). This is notably in contrast to the common assumptions of linear lapse rates (i.e., warmer temperatures at lower elevations) applied in most glacier melt models, suggesting a

Visualization: Thomas E. Shaw, Evan S. Miles

Writing – original draft: Thomas E. Shaw

Writing – review & editing: Thomas E. Shaw, Pascal Buri, Michael McCarthy, Evan S. Miles, Álvaro Ayala, Francesca Pellicciotti

systematic over-estimation of Ta under such warm atmospheric conditions (Carturan et al., 2015; Petersen & Pellicciotti, 2011; Shea & Moore, 2010).

Recent works have highlighted this problem in increasing detail with examples from on-glacier data sets around the world (Ayala et al., 2015; Carturan et al., 2015; Conway et al., 2021; T. Shaw et al., 2021; T. E. Shaw et al., 2017; Troxler et al., 2020; Yang et al., 2022). Several of those works have also identified the presence of warm air processes that generate increases in Ta toward the terminus of mountain glaciers (Ayala et al., 2015; T. E. Shaw et al., 2017; Troxler et al., 2020). Various hypotheses have been raised as to the cause of this behavior (e.g., debris warming, convergent and divergent air flows, valley winds). Moreover, detailed eddy-flux measurements (Nicholson & Stiperski, 2020), atmospheric model simulations (Potter et al., 2018), and large eddy simulations (Goger et al., 2022; Sauter & Galos, 2016) have highlighted those potential interactions of air masses with distinct trajectories for fine atmospheric conditions. Ultimately, the governing processes of on-glacier Ta variability will likely evolve as mountain glaciers continue to shrink and their boundary layers further diminish (Carturan et al., 2015; Jiskoot & Mueller, 2012). As such, the empirical relationships between temperature and ice melt rate may change as a result (e.g., Bolibar et al., 2022).

Due to the lack of long-term, distributed observations, however, no study to the authors' knowledge has explored the evolution of the on-glacier Ta through time and its response to atmospheric warming and glacier changes. Here we compile six distinct years of meteorological datasets on the Swiss Haut Glacier d'Arolla to explore the changing air temperature and wind patterns spanning 2001–2022. We aim to explore the following questions:

1. how variable is on-glacier Ta in space and time?
2. how has Ta responded to changing surface and meteorological conditions as the glacier diminishes?
3. what do these changes imply about the boundary layer development of decaying mountain glaciers?

2. Study Site

Haut Glacier d'Arolla (45.97°N, 7.52°E) is a small mountain glacier located in the southwestern Swiss Alps at the head of Val d'Herens, Canton Valais (Figure 1a). As of 2022, the glacier area was approximately 3.3 km², with supraglacial debris covering around 22% of the total surface area. The area of the glacier has reduced by ~35% since 2001, with more rapid frontal retreat and tributary separation since ~2005 (Figures 1a and 1b, Figure S1 in Supporting Information S1). Since the early 1990s, the glacier has been subject of numerous studies exploring surface conditions and energy balance (e.g., Brock et al., 2000; Carenzo, 2012; Strasser et al., 2004), subglacial hydrology and morphology (e.g., Nienow et al., 1998; Sharp et al., 1993), and glacier mass balance (e.g., Arnold et al., 1996; Dacic et al., 2008; Willis et al., 2002). Since 2010, distributed measurements of Ta and other energy balance variables have been used to explore some of the common assumptions regarding Ta distribution in melt modeling (Ayala et al., 2015; Petersen et al., 2013).

3. Data

The meteorological setup consists of on- and off-glacier air temperature stations (hereafter “T-Loggers”) and automatic weather stations (“AWS”). T-loggers are free-standing, 2 m tripods that support an Onset Tidbitv2 temperature logger (accuracy 0.2°C) housed in a naturally ventilated radiation shield. The type of radiation shield is distinct between the 2010 campaign (see Petersen and Pellicciotti (2011)) and that of 2021 and 2022 (see Section S3 in Supporting Information S1). AWS sensors vary given the year of study (see Table S3 in Supporting Information S1) but typically provide a full array of meteorological variables, including aspirated air temperature and humidity, wind speed and direction and radiative fluxes.

Before 2010, one pro-glacial AWS was operated by the Grand Dixence hydropower company (“OFF1” in Figure 1a—2,507 m a.s.l.), with an additional upper AWS available in 2010 (“OFF3”—2,985 m a.s.l.). In 2021 and 2022, a T-Logger was installed near to site “OFF3” at high elevation and in the pro-glacial zone (“OFF2”—2,531 m a.s.l.). OFF1 and OFF2 were >700 m from the terminus of the glacier in the respective year, suggested to be close to the limit of katabatic wind intrusion into the glacier forefield (Oke, 2002). Therefore, we use data from OFF1 (2001–2010) and OFF2 (2021–2022) to provide an indication of off-glacier, “ambient” air temperature (hereafter Ta_{OFF}). Data from the other off-glacier AWS were not available after 2010. Full details on AWS and T-Logger specifications are given in Table S3 in Supporting Information S1.

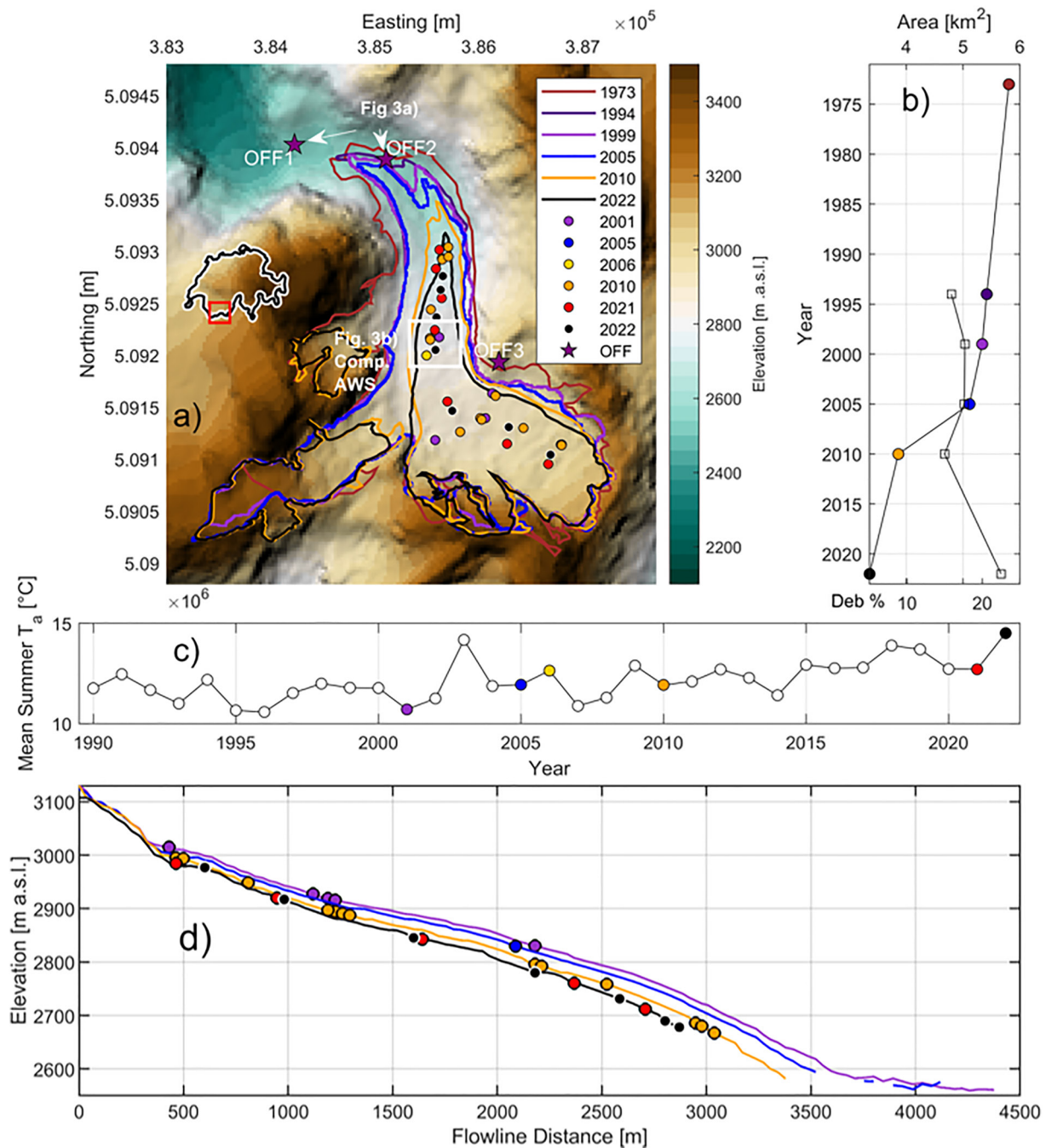


Figure 1. (a) The location and changing area of Haut Glacier d'Arolla through time, including the location of automatic weather stations and T-Logger measurements in each year. The location of off-glacier ("OFF"-Table S2 in Supporting Information S1) stations are provided and referred to in the main text. (b) The area of the glacier given by the available historic outlines (Table S1 in Supporting Information S1) and recently digitized extents (colored circles) and the debris cover percentage (hollow squares), as derived from Landsat imagery. (c) The mean summer (JJAS) T_a at the median glacier elevation of all years (2,960 m a.s.l.), extrapolated from the long-term temperature records of Zermatt weather station (1,638 m a.s.l.) using the ELR. The years of comparison are highlighted in the respective colors. (d) The elevation and extent of the glacier flowline in 4 years with digitized digital elevation models, where the station locations are indicated with circles. Colors for all subplots are as given in panel (a) legend.

Station data are filtered for obvious errors and extreme values are manually removed (e.g., when T-loggers fell over due to strong differential ablation or heavy storms—Figure S3 in Supporting Information S1). Due to the potential for naturally ventilated radiation shields to overheat and bias T_a measurements under high insolation, low wind speed conditions (Carturan et al., 2015; Cullen & Conway, 2015; Georges & Kaser, 2002), we compare

naturally and artificially aspirated Ta observations that were recorded at the same location (2010 and 2022). We utilize a multivariate-regression to estimate the hourly Ta differences (natural— aspirated) from hourly wind speed and incoming shortwave radiation measurements (Figure S4 in Supporting Information S1) and use this to correct the naturally ventilated Ta observations. Details on data corrections and uncertainties are described in Section S2 in Supporting Information S1. Spatial information related to glacier extent and hypsometry (Figure 1) are taken from historic and newly digitized data as described in Section S1 in Supporting Information S1.

4. Methods

4.1. Temperature Sensitivity

In order to estimate the state of the glacier boundary layer and its change through time, it is useful to consider the sensitivity of on-glacier Ta to the equivalent off-glacier Ta at a given elevation. This “temperature sensitivity” (TS) is defined as the ratio of the on-glacier observed Ta at each station (Ta_{obs}) to the above-zero estimated, off-glacier Ta at the same elevation (Ta_{est}) derived from the slope of the regression equation:

$$TS = \frac{Ta_{obs} - \beta}{Ta_{est}}, \quad (1)$$

Where β is the regression intercept and Ta_{est} is derived following:

$$Ta_{est} = Ta_{OFF} + \Gamma \cdot (Z_{obs} - Z_{OFF}), \quad (2)$$

where Γ refers to the hourly variable temperature lapse rate derived from all available off-glacier Ta records or the literature (see Section S2 in Supporting Information S1) and Z_{obs} and Z_{OFF} are the respective elevations of the on-glacier observation and OFF1/OFF2. A sensitivity of 1 indicates that a change in Ta_{obs} is equal to a change Ta_{est} and that no cooling in the glacier boundary layer (Carturan et al., 2015) is detectable (i.e., the air temperature on-glacier is equal to the one off-glacier at the same elevation). Conversely, a sensitivity of 0.5 would indicate that, on average, for every 1°C change in the off-glacier Ta, a 0.5°C change in observed on-glacier Ta is evident (an example is given in Figure S5 in Supporting Information S1). This is the same as presented by earlier works (Greuell & Böhm, 1998; J. Oerlemans, 2001) and similar to the statistical estimation framework presented by Shea and Moore (2010), which divides relative temperature changes on the glacier by a threshold event for the onset of katabatic conditions.

4.2. Data Subsets

To assess the influence of the valley wind system on Ta_{obs} , we define an up-valley/glacier wind index (UWI) that follows the form:

$$UWI = \cos\left(\frac{|DIR - \varphi| \cdot \pi}{180}\right), \quad (3)$$

where DIR is the wind direction (°) for a given hour and φ is the up-valley/glacier orientation (°). Accordingly, a value of one indicates that the wind direction is precisely up-valley/glacier and a value of negative one states that it is precisely down-valley/glacier. Changes in average UWI through time provide an indication of a wind regime switch at our study site. To emphasize the changes in on-glacier wind through the years, we compare selected stations on the glacier that have similar flowline distances (white box in Figure 1a—hereafter our “comparative AWS location”).

Finally, we analyze temperature sensitivity (TS—Equation 1) patterns by grouping observations by percentiles of Ta_{OFF} at OFF1 (2001–2010) or OFF2 (2021–2022). As warmer atmospheric conditions are associated with an increasing katabatic activity for many mountain glaciers, including Haut Glacier d’Arolla (Ayala et al., 2015; Petersen et al., 2013), we group all Ta_{obs} by the contemporaneous values of Ta_{OFF} above the 50th percentile of Ta at the off-glacier station (“P50”). To compare the response of the glacier to the same conditions between the years, we additionally calculate TS using a common range of positive air temperatures at OFF1/OFF2 (4°C–12°C).

4.3. Energy Balance Calculations

To explore the impact of katabatic boundary layer decay on the glacier, we calculate the point-based energy balance at the comparative AWS location (Figure 1a) using the cryospheric component of the land surface model

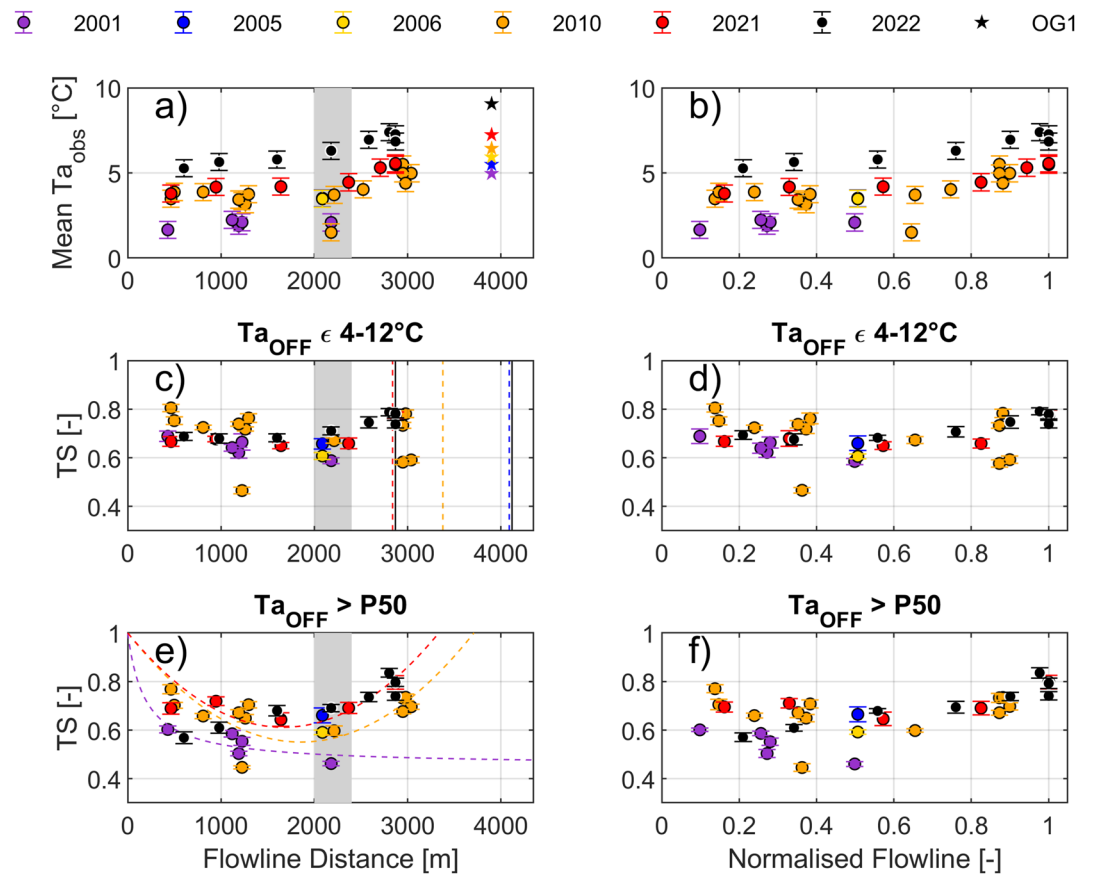


Figure 2. Mean air temperature profiles versus distance along (a) the glacier flowline (m) and (b) the normalized flowline. Panels (c–f) show the temperature sensitivity (“temperature sensitivity” (TS)—Equation 1) versus the distance along the flowline and normalized flowline for panels (c, d) the common ambient temperature range (4°C–12°C) and (e, f) the warmest 50% of ambient temperatures at OFF1/OFF2 (P50) in each year. Stars in panel (a) indicate the mean off-glacier air temperature at OFF1/OFF2. Vertical lines in panel (c) indicate terminus positions of individual years (2001 is at the max. x-axis limit). In panel (e), dashed lines highlight the fitted curves given a 0 m flowline start point (where TS theoretically = 1) and the observed data for 2001, 2010, and 2021 (the lower-most data point of 2021 is partly occluded). The theoretical lines in panel (e) follow the suggestions of previous works (e.g., Greuell & Böhm, 1998) that indicate a 1:1 temperature change at the top of a glacier (a crest or ice divide) where the glacier boundary layer does not exist or is negligible. The gray shaded box indicates the common flowline area of the glacier for later comparison of individual automatic weather stations measurements.

Tethys-Chloris (T&C) (Fatichi et al., 2012, 2021; Fugger et al., 2022). The model is run at an hourly resolution for the entire period of observation in each year (Figure S3 in Supporting Information S1) using a reconstructed meteorological time-series (see Section S5 in Supporting Information S1) and evaluated against ablation stake data (Figure S9 in Supporting Information S1).

5. Results

5.1. Patterns of Temperature and Temperature Sensitivity

There is evidence of increasing mean on-glacier T_a (Figure 2) consistent with warmer ambient conditions over the last decade (Figure 1c). While mean T_a has only slightly warmed at the glacier terminus between 2010 and 2021 (0.4°C increase >2,000 m along the flowline), 2022 temperatures are ~2.5°C warmer on average than 2021 and ~3°C warmer than the average pre-2010 T_a at 2,000–2,500 m flowline distance (Figure 2a). On-glacier T_a at the comparable AWS location (gray box in Figure 2a) have increased more relative to $T_{a,OFF}$ in recent years.

Irrespective of the year, temperature sensitivities (TS) typically decrease or remain stable until ~2,000 m along the glacier flowline, followed by increases toward the terminus of the glacier (Figures 2c and 2d). For a common

off-glacier temperature range (4°C–12°C), TS typically lowers to a minimum of ~ 0.6 before gently rising toward 3,000 m along the flowline (Figure 2c), with slightly higher TS (0.75) in 2021 and 2022. For warmer atmospheric conditions ($T_{a\text{OFF}} > P50$), the contrast between earlier and later years is stronger (Figure 2e) with a more pronounced decrease of TS toward the mid-glacier for earlier years, followed by a relative increase in TS beyond 2,000 m in the later years. Comparing observations from 2010 onward, TS on the lower terminus has increased, by >0.07 on average between 2010 and 2021, and by >0.09 on average between 2010 and 2022 (Figure 2e). Although observations do not extend to the glacier terminus for 2001 (Figure 1a), comparable observations at 2,000–2,400 m (gray boxes in Figure 2) demonstrate a clear change in the relationship of TS to the glacier flowline. Given a normalized flowline distance between the headwall and glacier terminus in each year, TS closely relates to the proximity of observations to the glacier terminus (Figure 2f).

5.2. Evolution of Glacier and Valley Winds

Observations show an increasing fraction of up-valley winds (increasingly positive UWI) at OFF1 (2001–2010) and OFF2 (2021 and 2022) for the afternoon-evening hours, steadily increasing since 2001 and rising by $>20\%$ between 2001 and 2021 for 12:00–19:00 (Figure 3a), though 2022 is more similar to 2010. Nighttime patterns show less of a trend through time, and highlight the typical nocturnal katabatic drainage associated with mountain environments. Up-glacier winds (UWI for the on-glacier AWS location) also increased for late afternoon hours since 2001, with UWI becoming more positive even for 2005 and 2006 (Figure 3b), possibly linked to the rapidly decreasing glacier frontal area in the period 2005–2010 (Figure 1b). The warm conditions of 2022 show a strong occurrence of up-glacier winds between 12:00–21:00 (mean UWI > 0.4) and a nocturnal down-glacier flow, whereas 2021 saw a dominance of up-glacier winds for most hours, despite winds being weaker (Figure S6 in Supporting Information S1).

5.3. Relation of Temperature Sensitivity to Wind

Considering the comparable AWS on the glacier (Figure 1a—white box, Figure 2a—gray box, Table S3 in Supporting Information S1) a clear change in the relation between warm conditions and the occurrence of katabatic winds is evident (Figures 3c–3h). For the summers of 2001–2010, warm conditions are mostly associated with the occurrence of down-glacier winds (negative UWI), whereas up-glacier wind conditions are mostly associated with synoptic storm events (Strasser et al., 2004) and under cooler ambient conditions with high fractional snow coverage on the glacier (Figures 3c–3f). 2021 and 2022 see an increased occurrence of up-valley winds for the entire range of positive temperatures, contrasting with the conventional expectation for katabatic wind development. For the common positive temperature range in all years, mean daily UWI increased from -0.6 between 2001 and 2010 (Figures 3c–3f), to ~ 0.05 in 2021 and 2022 (Figures 3g and 3h). For 2022, snow was almost completely absent from the glacier (Figure S7 in Supporting Information S1), whereas 2021 experienced up-valley winds under a range of snow-cover conditions, thus discounting snow presence as a dominant control in the following analysis.

Figures 3i–3k shows the inter-annual profiles of TS related to the direction of winds for warm ambient conditions ($T_{a\text{OFF}} > P50$). Down-glacier winds are accompanied by a decrease and subsequent increase of sensitivity (Figure 2e) for 2010–2022. For the comparable AWS location on the glacier (Figure 1a), TS is 36%–58% greater for 2010–2022 under the presence of katabatic winds, in comparison to the pre-2010 period (Figure 3i). Up-glacier wind occurrence produces consistently higher TS across the glacier for all years and across most of the flowline (Figure 3j), highlighting the expected erosion of the katabatic boundary layer for warm, up-glacier winds (e.g., Petersen & Pellicciotti, 2011; T. Shaw et al., 2021). In 2022, up-valley winds notably establish a decreasing TS with distance up-glacier (Figure 3j), likely due to a combination of adiabatic cooling and sensible heat loss as air moves up-glacier to the highest elevations. This also acts to re-establish the elevation-dependence of on-glacier temperatures for 2022, such that a lapse rate could appropriately describe on-glacier temperature variability under warm atmospheric conditions (Figure S8 in Supporting Information S1). Wind mixing events (coincident down-glacier and up-valley winds) result in a similar pattern to completely down-glacier/down valley wind events (Figure 3k), though most years have too few observations to robustly test the resulting TS.

5.4. Relevance of Decay to Surface Energy Balance

Since 2010, up-valley winds have become the dominant contributor to sensible heat fluxes on the glacier (Figure 4). Prior to 2021, the majority of up-valley winds occurred only under cooler ambient conditions (Figures 3c–3e), though contributed similarly to the sensible heat flux on the glacier due to stronger winds (Figures 4a and 4b). In

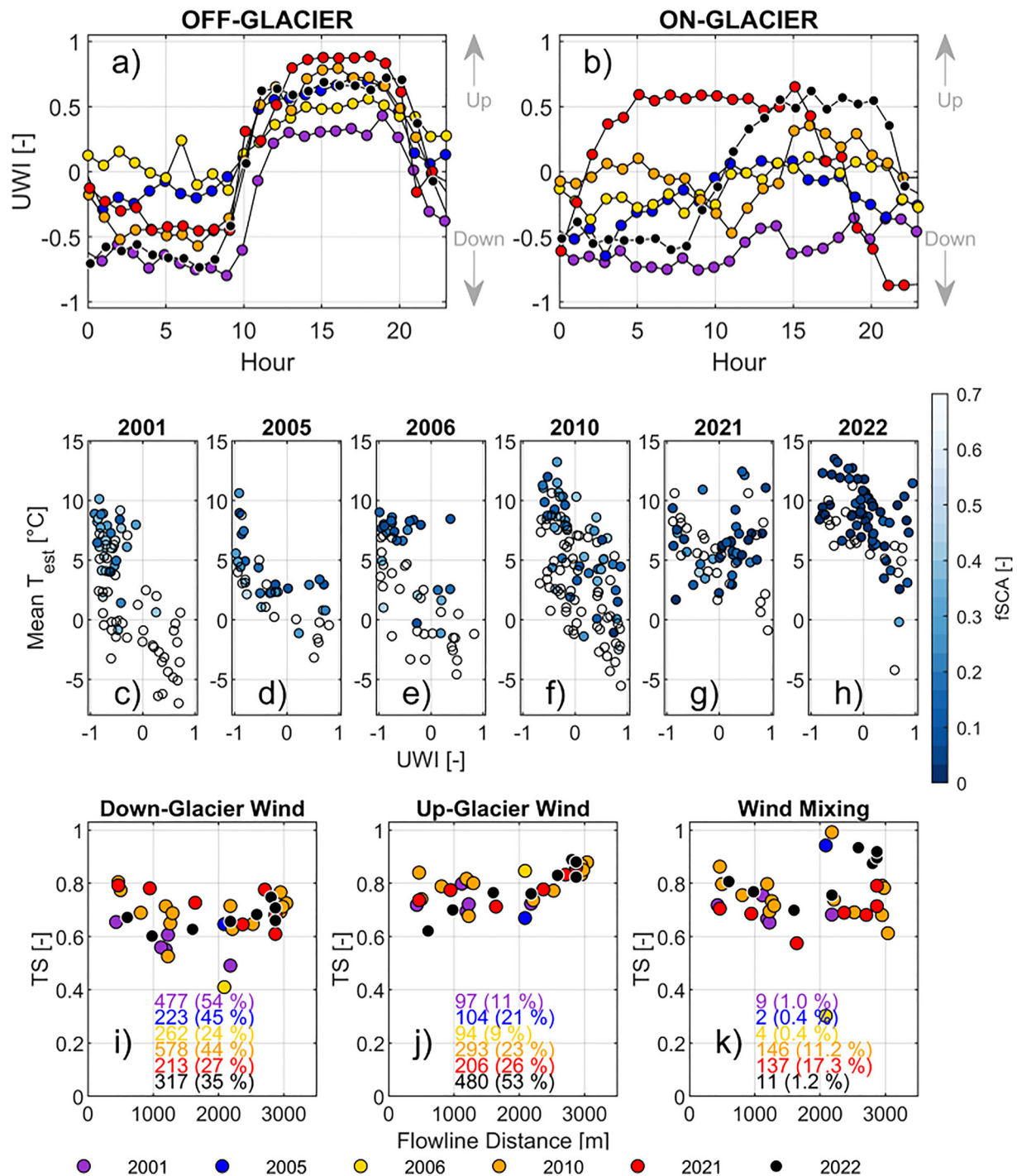


Figure 3. Panels (a, b) show the (a) mean diurnal off- and (b) on-glacier up-valley/glacier wind index (up-valley/glacier wind index [UWI]—see Equation 3) per year for the period of observation. The on-glacier observations from the comparative automatic weather stations location as indicated in Figure 1a show the daily mean estimated ambient temperature (Equation 2) at the elevation of the mid-flowline observation point (gray box in Figure 2a) and the mean daily UWI (Equation 3) colored by the glacier-wide fractional snow-covered area derived from MODIS MOD10A1 (Figure S7 in Supporting Information S1) for each year of observation. Panels (i–k) show the temperature sensitivity profiles versus along flowline distance (m) given $T_{a,OFF} > P50$ conditions (Figure 2e) that experience (i) only down-glacier (and down-valley) wind, (j) only up-glacier (and up-valley) wind, and (k) down-glacier, but up-valley wind, whereby mixing may occur somewhere on, or near to the glacier terminus. The number of hourly observations and percentage of the total for each case in each year (colors) are given by the inset text. Up (down) valley winds are those with a positive (negative) UWI where wind speeds exceed 1 m s^{-1} .

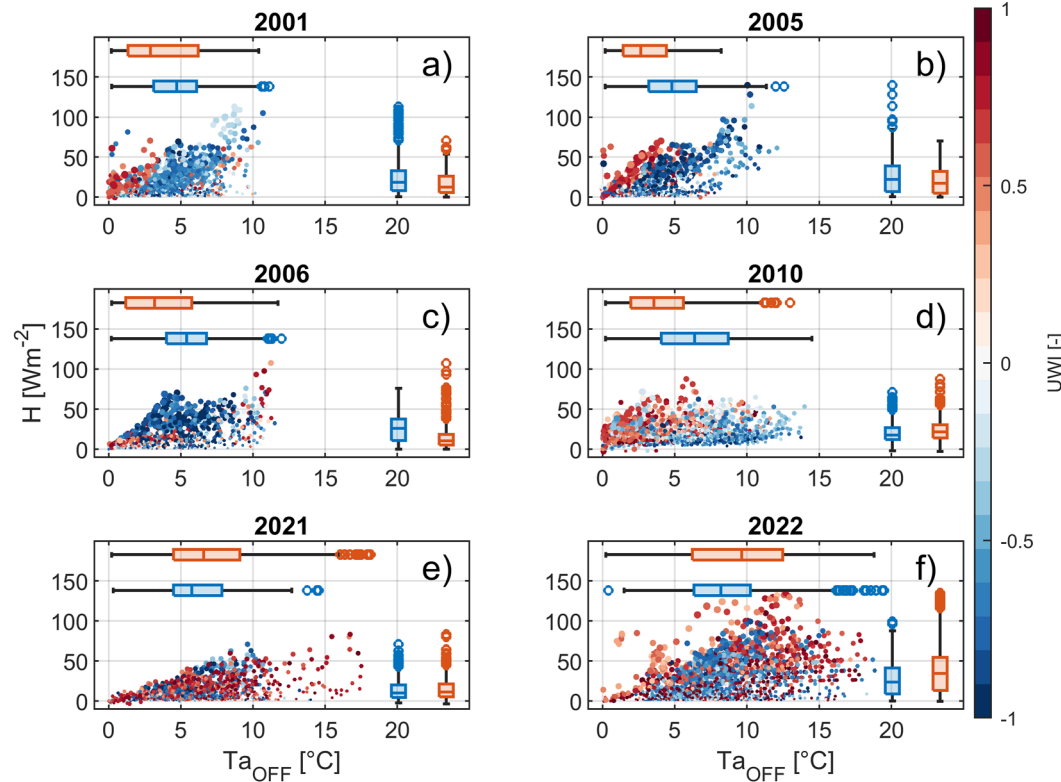


Figure 4. Modeled instantaneous sensible heat fluxes (H) at the comparable on-glacier station location (Figure 1a) as a function of ambient, off-glacier air temperature in each year (positive values only). Scatter plots are colored by the on-glacier up-valley/glacier wind index (UWI), whereby reds indicate an up-glacier wind direction, and the size is scaled by measured on-glacier wind speed (values above 1 m s^{-1} are considered). Inset boxplots for each panel indicate the distributions of H (vertical boxplots) and Ta_{OFF} (horizontal boxplots) in each year, sub-divided by predominantly up(down)-glacier winds in red(blue). Up(down)-glacier winds were classified as those greater(less) than 0 UWI. Model details are provided in Section S5 in Supporting Information S1.

these earlier years, only katabatic winds (negative UWI), forming under warm ambient conditions, produced sensible heat flux to the surface exceeding 70 W m^{-2} . After 2005, larger reductions in the terminus extent (Figure 1) coincided with a wind regime shift, such that up-valley winds were increasingly responsible for producing the larger sensible heat fluxes (boxplots of Figures 4c–4f). Moreover, in 2021 and 2022, median off-glacier temperatures under down-glacier winds became lower than under up-valley winds (boxplots in Figures 4e and 4f). 2022 was characterized by record breaking warm weather, following a dry winter (Cremona et al., 2022), resulting in large fluxes of sensible energy to the surface given strong up-valley winds under a range of ambient temperatures (Figure 4f, Figure S10 in Supporting Information S1). During 2022, mean sensible heat flux under up-glacier wind conditions is 43% greater than that which coincided with down-glacier winds, while sensible heat flux is 54% less on average during up-glacier winds pre-2010 (Figure 4, Table S4 in Supporting Information S1).

6. Discussion

A tendency toward more physically based modeling of glaciers (e.g., Y. Wang et al., 2021) increases the dependence on accurate forcing data (Gabbi et al., 2014), as forcing data errors are less able to be compensated during parameter calibration. Within the context of glacier meteorology, much work has been done to explore the spatial and temporal variability of near-surface air temperature and wind fields and its role in the decoupling of the glacier boundary layer with its surroundings (Ayala et al., 2015; Conway et al., 2021; Greuell & Böhm, 1998; Shea & Moore, 2010; Yang et al., 2022). However, while the key physical processes determining katabatic development are well understood (e.g., B. J. Oerlemans & Grisogono, 2002; Van Den Broeke, 1997), most studies have only provided a perspective at individual points on a glacier ablation zone and often for an individual year.

A key finding of our study is the increased incursion of up-valley winds into the glacier boundary layer, accompanied by increased frequency of warmer conditions on the glacier. In the past, warm conditions generated down-glacier katabatic winds (Strasser et al., 2004), whereas now warm conditions are mostly associated with external up-valley winds. In line with the hypotheses of Carturan et al. (2015), our observations have demonstrated for the first time, to the authors' knowledge, the increasing sensitivity of the above-ice air temperatures to external climate as a mountain glacier shrinks and fragments. This has interesting implications for future glacier modeling (e.g., Figure 4) given the expected feedback of an increased sensitivity to external warming due to a lack of boundary layer development that is further diminished due to glacier mass loss and retreat. Under the same ambient temperature range, the increase in sensitivity at the same distance down-glacier is modest (Figure 2c), though as the glacier retreats and debris cover expands, more area is exposed to the presence of warm air (Figure 2d). Moreover, as the katabatic activity ceases to develop on a glacier of such size (Carturan et al., 2015; T. Shaw et al., 2021), the dependency of temperature on elevation (and the applicability of a lapse rate) is restored (Figure S8 in Supporting Information S1), emphasizing a further non-linearity of glacier response to climatic warming.

Given that negligible differences in topographically induced convergence/divergence of down-glacier air would be expected between the years (Munro, 2006) and that turbulence driven by wind interactions from down-glacier and up-valley source regions are uncommon (Figure 3k), the dominant source of this increased sensitivity appears to be linked to the increase in up-valley/glacier winds (Figure 3) entraining warmer air which passes over snow-free terrain and an expanding debris-covered area (Figure 1b). While there is clearly an increasing temperature deficit between the atmosphere and near-surface required to generate katabatic winds (Figure 1c), the glacier fetch is seemingly no longer sufficient to overcome the valley circulation and slope winds generated by warm and dry conditions in recent years (Greuell & Böhm, 1998; Potter et al., 2018).

The variability in temperature sensitivity for down-glacier wind events under warm conditions (Figure 3i) suggests the role of heat advection from snow-free slopes (Haugeneder et al., 2022; Mott et al., 2018, 2020) in drier years such as 2010 and 2022. For those snow-dominated years (2001, 2006, and 2021), cold air drainage was seemingly more efficient, producing the less temperature sensitive conditions at lower elevations (Figure 3i), and adhering to the patterns described for larger glaciers in earlier works (Greuell & Böhm, 1998; Shea & Moore, 2010). However, the absolute differences in temperature sensitivity at the shortest flowline distances (Figures 2e and 3i) remain to be explained and could likely implicate many local effects (T. E. Shaw et al., 2017; Strasser et al., 2004) that are not resolved here.

Previous work addressing air temperature distribution on multiple glaciers (Carturan et al., 2015; T. Shaw et al., 2021; Shea & Moore, 2010; Yang et al., 2022) have highlighted the need to account for different glacier characteristics (principally glacier length) when forcing fully distributed, physically based or intermediate complexity (ETI) models of snow and ice melt (Carturan et al., 2015; Petersen & Pellicciotti, 2011; T. E. Shaw et al., 2017). Our analyses are limited due to the variable location of on-glacier stations and due to a short total observational period, despite a notable retreat of the Arolla Glacier in the last 20 years (Figure 1). Nevertheless, our work presents novel evidence as to the necessity of an appropriate temperature distribution parameterization that explicitly accounts for the non-linear changes in sensitivity of the glacier through time (e.g., Bolibar et al., 2022). The inclusion of feedbacks related to reduced katabatic wind speeds (Figure 4) and adjustment of vapor pressure gradients (Shea & Moore, 2010) would also be of great relevance for future glacier and glacio-hydrological modeling at local/sub-regional scales. Further work to establish critical length scales associated with this shift in wind regime would be beneficial, particularly because as much as half of the world's mountain glaciers are expected to disappear by the end of the century based upon recent modeling estimates (Rounce et al., 2023).

7. Conclusions

We have demonstrated novel instrumental evidence as to the decay of katabatic winds on a small, shrinking Alpine glacier by exploring on- and off-glacier meteorological data for six years in the period 2001–2022. The glacier lost ~35% of its area since 2001, coinciding with notable frontal retreat post 2005, warming temperatures on the glacier and an increase in the occurrence of up-valley/glacier winds on the glacier. An increase in up-valley slope flows permitted by the decay of the katabatic boundary layer has promoted an increased intrusion of warm air flowing up the glacier during the summer, increasing the sensitivity of on-glacier air temperatures to external climate and reestablishing the applicability of lapse rates to describe its variability. Moreover, the retreat of

the glacier terminus and increased presence of supraglacial debris cover acts to increase the area of the glacier that is sensitive to off-glacier temperature changes. Accordingly, sensible heat fluxes to the glacier are increasingly determined by the conditions occurring outside the boundary layer of the glacier. Ultimately, the enhanced sensitivity of on-glacier near-surface temperatures to external environmental conditions implies an accelerated negative response of glacier melt to climate warming, partly explaining the observed non-linear decay of alpine glaciers.

Acronyms

Ta	Near-surface air temperature
TS	Temperature sensitivity
OFF(n)	An off-glacier observation location
Ta _{OFF}	The off-glacier Ta at the off-glacier station of the given year
Ta _{obs}	Observed Ta at station locations on the glacier
Ta _{est}	Ta estimated for the elevation of Ta _{obs} based upon observations from OG and a calculated lapse rate
Z _{OFF}	The elevation of the OFF station
Z _{obs}	The elevation of the on-glacier station observations Ta _{obs}
P50	The 50th percentile of Ta at the off-glacier station

Data Availability Statement

The meteorological data used in this analysis (T. E. Shaw et al., 2023) are made publicly available at the following repository: <https://doi.org/10.5281/zenodo.7554648>. The source code of the T&C model is available at <https://doi.org/10.24433/CO.0905087.v2>.

Acknowledgments

This work was funded by the EU Horizon 2020 Marie Skłodowska-Curie Actions Grant 101026058. The authors acknowledge the dedicated collection of field data by many parties since 2001, including those acknowledged for the cited works on Arolla Glacier. The authors would like to thank Fabienne Meier, Alice Zaugg, Raphael Willi, Maria Grundmann, and Marta Corrà for assistance in the field for the summers of 2021 and 2022. Off-glacier data provided by Grand Dixence SA (Arolla) and MeteoSwiss are kindly acknowledged. Simone Faticchi is thanked for the provision and support in the use of the Tethys-Chloris model. We thank Editor Mathieu Morlighem and two anonymous reviewers whose comments have helped to improve the quality of the manuscript.

References

- Arnold, N. S., Willis, L. C., Sharp, M. J., & Richards, K. S. (1996). A distributed surface energy-balance model for a small valley glacier. *Journal of Glaciology*, 1(82).
- Ayala, A., Pellicciotti, F., & Shea, J. (2015). Modeling 2m air temperatures over mountain glaciers: Exploring the influence of katabatic cooling and external warming. *Journal of Geophysical Research: Atmospheres*, 120(8), 1–19. <https://doi.org/10.1002/2015JD023137>. Received
- Bolíbar, J., Rabatel, A., Gouttevin, I., Zekollari, H., & Galiez, C. (2022). Nonlinear sensitivity of glacier mass balance to future climate change unveiled by deep learning. *Nature Communications*, 13(1), 1–11. <https://doi.org/10.1038/s41467-022-28033-0>
- Brock, B. W., Willis, I. C., & Sharp, M. J. (2000). Measurement and parameterization of albedo variations at Haut Glacier d'Arolla, Switzerland. *Journal of Glaciology*, 46(155), 675–688. <https://doi.org/10.3189/172756500781832675>
- Carenzo, M. (2012). *Distributed modelling of changes in glacier mass balance and runoff*. (Unpublished doctoral dissertation). ETH Zurich.
- Carturan, L., Cazorzi, F., De Blasi, F., & Dalla Fontana, G. (2015). Air temperature variability over three glaciers in the Ortles–Cevedale (Italian Alps): Effects of glacier fragmentation, comparison of calculation methods, and impacts on mass balance modeling. *The Cryosphere*, 9(3), 1129–1146. <https://doi.org/10.5194/tc-9-1129-2015>
- Chen, Y., Li, W., Fang, G., & Li, Z. (2017). Review article: Hydrological modeling in glacierized catchments of central Asia—status and challenges. *Hydrology and Earth System Sciences*, 21(2), 669–684. <https://doi.org/10.5194/hess-21-669-2017>
- Conway, J., Helgason, W., Pomeroy, J., & Sicart, J. (2021). Icefield breezes: Mesoscale diurnal circulation in the atmospheric boundary layer over an outlet of the Columbia Icefield, Canadian Rockies. *Journal of Geophysical Research: Atmospheres*, 126(6), 1–17. <https://doi.org/10.1029/2020jd034225>
- Cremona, A., Huss, M., Landmann, J. M., Borner, J., & Farinotti, D. (2022). Heat wave contribution to 2022's extreme glacier melt from automated real-time ice ablation readings (pp. 1–27).
- Cullen, N. J., & Conway, J. P. (2015). A 22 month record of surface meteorology and energy balance from the ablation zone of Brewster Glacier, New Zealand. *Journal of Glaciology*, 61(229), 931–946. <https://doi.org/10.3189/2015JoG15J004>
- Dadic, R., Corripio, J. G., & Burlando, P. (2008). Mass-balance estimates for Haut Glacier d'Arolla, Switzerland, from 2000 to 2006 using DEMs and distributed mass-balance modeling. *Annals of Glaciology*, 49, 22–26. <https://doi.org/10.3189/172756408787814816>
- Faticchi, S., Ivanov, V. Y., & Caporali, E. (2012). A mechanistic ecohydrological model to investigate complex interactions in cold and warm water-controlled environments: 2. Spatiotemporal analyses. *Journal of Advances in Modeling Earth Systems*, 4(5), M05002. <https://doi.org/10.1029/2011MS000087>
- Faticchi, S., Peleg, N., Mastrotheodoros, T., Pappas, C., & Manoli, G. (2021). An ecohydrological journey of 4500 years reveals a stable but threatened precipitation-groundwater recharge relation around Jerusalem. *Science Advances*, 7(37), 1–9. <https://doi.org/10.1126/sciadv.abe6303>
- Fugger, S., Fyffe, C. L., Faticchi, S., Miles, E., McCarthy, M., Shaw, T. E., et al. (2022). Understanding monsoon controls on the energy and mass balance of glaciers in the Central and Eastern Himalaya. *The Cryosphere*, 16(5), 1631–1652. <https://doi.org/10.5194/tc-16-1631-2022>
- Gabbi, J., Carenzo, M., Pellicciotti, F., Bauder, A., & Funk, M. (2014). A comparison of empirical and physically based glacier surface melt models for long-term simulations of glacier response. *Journal of Glaciology*, 60(224), 1140–1154. <https://doi.org/10.3189/2014JoG14J011>
- Georges, C., & Kaser, G. (2002). Ventilated and unventilated air temperature measurements for glacier-climate studies on a tropical high mountain site. *Journal of Geophysical Research*, 107(D24), 4775. <https://doi.org/10.1029/2002JD002503>

- Goger, B., Stiperski, I., Nicholson, L., & Sauter, T. (2022). Large-eddy simulations of the atmospheric boundary layer over an Alpine glacier: Impact of synoptic flow direction and governing processes. *Quarterly Journal of the Royal Meteorological Society*, *148*(744), 1319–1343. <https://doi.org/10.1002/qj.4263>
- Greuell, W., & Böhm, R. (1998). 2 m temperatures along melting mid-latitude glaciers, and implications for the sensitivity of the mass balance to variations in temperature. *Journal of Glaciology*, *44*(146), 9–20. <https://doi.org/10.3189/s002214300002306>
- Greuell, W., Knap, W. H., & Smeets, P. C. (1997). Elevational changes in meteorological variables along a midlatitude glacier during summer. *Journal of Geophysical Research*, *102*(D22), 25941–25954. <https://doi.org/10.1029/97JD02083>
- Haugeneder, M., Lehning, M., Reynolds, D., Jonas, T., & Mott, R. (2022). A novel method to quantify near-surface boundary-layer dynamics at ultra-high spatio-temporal resolution. *Boundary-Layer Meteorology*, *186*(2), 177–197. <https://doi.org/10.1007/s10546-022-00752-3>
- Hock, R. (2005). Glacier melt: A review of processes and their modelling. *Progress in Physical Geography*, *29*(3), 362–391. <https://doi.org/10.1191/0309133305pp453ra>
- Immerzeel, W. W., Petersen, L., Ragetti, S., & Pellicciotti, F. (2014). The importance of observed gradients of air temperature and precipitation for modeling runoff from a glacierized watershed. *Water Resources Research*, *50*(3), 2212–2226. <https://doi.org/10.1002/2013WR014506>
- Received
- Jiskoot, H., & Mueller, M. S. (2012). Glacier fragmentation effects on surface energy balance and runoff: Field measurements and distributed modelling. *Hydrological Processes*, *26*(12), 1861–1875. <https://doi.org/10.1002/hyp.9288>
- Jouberton, A., Shaw, T. E., Miles, E. S., McCarthy, M. J., Fugger, S., Ren, S., et al. (2022). Warming-induced monsoon precipitation phase change intensifies glacier mass loss in the southeastern Tibetan Plateau. *Proceedings of the National Academy of Sciences of the United States of America*, *119*(37), 1–7. <https://doi.org/10.1073/pnas.2109796119>
- Karki, R., ul Hasson, S., Schickhoff, U., Scholten, T., Böhner, J., & Gerlitz, L. (2020). Near surface air temperature lapse rates over complex terrain: A WRF based analysis of controlling factors and processes for the central Himalayas. *Climatic Dynamics*, *54*(1–2), 329–349. <https://doi.org/10.1007/s00382-019-05003-9>
- Litt, M., Shea, J., Wagnon, P., Steiner, J., Koch, I., Stigter, E., & Immerzeel, W. (2019). Glacier ablation and temperature indexed melt models in the Nepalese Himalaya. *Scientific Reports*, *9*(1), 5264. <https://doi.org/10.1038/s41598-019-41657-5>
- Mölg, T., Maussion, F., Yang, W., & Scherer, D. (2012). The footprint of Asian monsoon dynamics in the mass and energy balance of a Tibetan glacier. *The Cryosphere*, *6*(6), 1445–1461. <https://doi.org/10.5194/tc-6-1445-2012>
- Mott, R., Stiperski, I., & Nicholson, L. (2020). Spatio-temporal flow variations driving heat exchange processes at a mountain glacier. *The Cryosphere*, *14*(12), 4699–4718. <https://doi.org/10.5194/tc-14-4699-2020>
- Mott, R., Vionnet, V., & Grünwald, T. (2018). The seasonal snow cover dynamics: Review on wind-driven coupling processes. *Frontiers of Earth Science*, *6*, 197. <https://doi.org/10.3389/feart.2018.00197>
- Munro, D. S. (2006). Linking the weather to glacier hydrology and mass balance at Peyto glacier (Tech. Rep.).
- Nicholson, L., & Stiperski, I. (2020). Comparison of turbulent structures and energy fluxes over exposed and debris-covered glacier ice. *Journal of Glaciology*, *66*(258), 1–3. <https://doi.org/10.1017/jog.2020.23>
- Nienow, P., Sharp, M., & Willis, I. A. N. (1998). Seasonal changes in the morphology of the subglacial drainage system, Haut Glacier d'Arolla, Switzerland. *Earth Surface Processes and Landforms*, *23*(9), 825–843. [https://doi.org/10.1002/\(sici\)1096-9837\(199809\)23:9<825::aid-esp893>3.0.co;2-2](https://doi.org/10.1002/(sici)1096-9837(199809)23:9<825::aid-esp893>3.0.co;2-2)
- Oerlemans, B. J., & Grigolon, B. (2002). Glacier winds and parameterisation of the related surface heat fluxes. *Tellus*, *54*(5), 440–452. <https://doi.org/10.1034/j.1600-0870.2002.201398.x>
- Oerlemans, J. (2001). *Glaciers and climate change*. AA Balkema.
- Oke, T. (2002). *Boundary layer climates*. Cambridge University Press.
- Petersen, L., & Pellicciotti, F. (2011). Spatial and temporal variability of air temperature on a melting glacier: Atmospheric controls, extrapolation methods and their effect on melt modeling, Juncal Norte Glacier, Chile. *Journal of Geophysical Research*, *116*(D23), D23109. <https://doi.org/10.1029/2011JD015842>
- Petersen, L., Pellicciotti, F., Juszak, I., Carenzo, M., & Brock, B. (2013). Suitability of a constant air temperature lapse rate over an Alpine glacier: Testing the Greuell and Böhm model as an alternative. *Annals of Glaciology*, *54*(63), 120–130. <https://doi.org/10.3189/2013AoG63A477>
- Potter, E. R., Orr, A., Willis, I. C., Bannister, D., & Salerno, F. (2018). Dynamical drivers of the local wind regime in a Himalayan valley. *Journal of Geophysical Research: Atmospheres*, *123*(23), 13186–13202. <https://doi.org/10.1029/2018JD029427>
- Ragetti, S., Immerzeel, W. W., & Pellicciotti, F. (2016). Contrasting climate change impact on river flows from high-altitude catchments in the Himalayan and Andes Mountains. *Proceedings of the National Academy of Sciences of the United States of America*, *113*(33), 9222–9227. <https://doi.org/10.1073/pnas.1606526113>
- Rounce, D., Hock, R., Maussion, F., Hugonnet, R., Kochitzky, W., Huss, M., et al. (2023). Global glacier change in the 21st century: Every increase in temperature matters David. *Science*, *83*, 78–83. <https://doi.org/10.1126/science.abo1324>
- Sauter, T., & Galos, S. P. (2016). Effects of local advection on the spatial sensible heat flux variation on a mountain glacier. *The Cryosphere*, *10*(6), 2887–2905. <https://doi.org/10.5194/tc-10-2887-2016>
- Scherrer, S. C. (2020). Temperature monitoring in mountain regions using reanalyses: Lessons from the Alps. *Environmental Research Letters*, *15*(4), 44005. <https://doi.org/10.1088/1748-9326/ab702d>
- Sharp, M., Richards, K., Willis, I., Arnold, N., Nienow, P., Lawson, W., & Tison, J. ä. (1993). Geometry, bed topography and drainage system structure of the haut glacier d'Arolla, Switzerland. *Earth Surface Processes and Landforms*, *18*(6), 557–571. <https://doi.org/10.1002/esp.3290180608>
- Shaw, T., Yang, W., Ayala, Á., Bravo, C., Zhao, C., & Pellicciotti, F. (2021). Distributed summer air temperatures across mountain glaciers in the south-east Tibetan Plateau: Temperature sensitivity and comparison with existing glacier datasets. *The Cryosphere*, *15*(2), 595–614. <https://doi.org/10.5194/tc-2020-198>
- Shaw, T. E., Brock, B. W., Ayala, A., Rutter, N., & Pellicciotti, F. (2017). Centreline and cross-glacier air temperature variability on an Alpine glacier: Assessing temperature distribution methods and their influence on melt model calculations. *Journal of Glaciology*, *63*(242), 1–16. <https://doi.org/10.1017/jog.2017.65>
- Shaw, T. E., Buri, P., McCarthy, M., Miles, E. S., Ayala, Á., & Pellicciotti, F. (2023). On-glacier meteorological data for Haut Glacier d'Arolla, Switzerland [Dataset]. Zenodo. <https://doi.org/10.5281/zenodo.7554648>
- Shea, J. M., & Moore, R. D. (2010). Prediction of spatially distributed regional-scale fields of air temperature and vapor pressure over mountain glaciers. *Journal of Geophysical Research*, *115*(D23), D23107. <https://doi.org/10.1029/2010JD014351>
- Sicart, J. E., Hock, R., & Six, D. (2008). Glacier melt, air temperature, and energy balance in different climates: The Bolivian Tropics, the French Alps, and northern Sweden. *Journal of Geophysical Research*, *113*(24), 1–11. <https://doi.org/10.1029/2008JD010406>

- Strasser, U., Corripio, J. G., Pellicciotti, F., Burlando, P., Brock, B. W., & Funk, M. (2004). Spatial and temporal variability of meteorological variables at Haut Glacier d'Arolla (Switzerland) during the ablation season 2001: Measurements and simulations. *Journal of Geophysical Research*, *109*(D3), D03103. <https://doi.org/10.1029/2003JD003973>
- Troxler, P., Ayala, Á., Shaw, T. E., Nolan, M., Brock, B. W., & Pellicciotti, F. (2020). Modelling spatial patterns of near-surface air temperature over a decade of melt seasons on McCall Glacier, Alaska. *Journal of Glaciology*, *1–15*(257), 386–400. <https://doi.org/10.1017/jog.2020.12>
- Van Den Broeke, M. R. (1997). Momentum, heat, and moisture budgets of the katabatic wind layer over a midlatitude Glacier in summer. *Journal of Applied Meteorology*, *36*(1987), 763–774. [https://doi.org/10.1175/1520-0450\(1997\)036<0763:mhambo>2.0.co;2](https://doi.org/10.1175/1520-0450(1997)036<0763:mhambo>2.0.co;2)
- Wang, X., Tolksdorf, V., Otto, M., & Scherer, D. (2020). WRF-based dynamical downscaling of ERA5 reanalysis data for High Mountain Asia: Towards a new version of the High Asia Refined analysis. *International Journal of Climatology*, *41*, 1–20. <https://doi.org/10.1002/joc.6686>
- Wang, Y., Wang, L., Zhou, J., Yao, T., Yang, W., Zhong, X., et al. (2021). Vanishing glaciers at Southeast Tibetan Plateau have not offset the declining runoff at Yarlung Zangbo. *Geophysical Research Letters*, *48*(21), e2021GL094651. <https://doi.org/10.1029/2021GL094651>
- Willis, I. C., Arnold, N. S., & Brock, B. W. (2002). Effect of snowpack removal on energy balance, melt and runoff in a small supraglacial catchment. *Hydrological Processes*, *16*(14), 2721–2749. <https://doi.org/10.1002/hyp.1067>
- Yang, W., Zhu, M., Guo, X., & Zhao, H. (2022). Air temperature variability in high-elevation glacierized regions: Observations from six catchments on the Tibetan Plateau. *Journal of Applied Meteorology and Climatology*, *61*(3), 1–35. <https://doi.org/10.1175/jamc-d-21-0122.1>